

Mean field study of 2D quasiparticle condensate formation in non-Markovian regime

N.A. Asriyan¹, A.A. Elistratov¹, and Yu.E. Lozovik^{2,3}

¹N.L. Dukhov Research Institute of Automatics (VNIIA), Moscow 127055, Russia;

²Institute for Spectroscopy RAS, Troitsk 108840, Moscow, Russia

³Moscow Institute of Electronics and Mathematics, National Research University Higher School of Economics, 101000 Moscow, Russia;

Bose-condensation in a system of 2D quasiparticles is considered in the scope of a microscopic model. Mean-field dynamical equations are derived with the help of the Schwinger-Keldysh formalism. We show that the main features of condensate interaction with the reservoir of non-condensed particles may be captured by a simple memory term with an exponential kernel. By analysing stationary solutions of this equation, we obtain the phase diagram of quasiparticle gas, finding a bistability region in the parameter space of the system. Finally, as an application of our theory, we study the phase diagram of exciton-polariton condensate.

1 Introduction

Decades after Bose-Einstein condensation was predicted theoretically [1, 2], it was observed directly in experiments with cold atoms in 1995 [3–5]. This observation was followed by discovering Bose-condensates in many other systems such as quantum well excitons [6, 7], exciton-polaritons [8, 9], magnons [10] and microcavity photons [11].

Though during condensate formation the cold atom gas is out of equilibrium, the resulting condensate state is an equilibrium one, which is not the case for solid state quasiparticle systems. Despite the similar nature of the low-temperature state in these systems and in cold atomic gases, the quasiparticle condensate is different in several aspects. Firstly, due to finite lifetime, these systems need to be pumped externally, hence the condensate is in a quasi-equilibrium state which is determined by an interplay between pumping and decay processes. Moreover, these condensates are often considered in low dimensional systems and together with small masses of quasiparticles, it may change totally the relevant scales (energies, times) of the condensate and the process of its formation. One of the most attractive features is the potential ability to observe high temperature condensation.

The basic Gross-Pitaevskii equation, describ-

ing condensate in equilibrium systems has been modified in numerous ways (leading to dissipative Gross-Pitaevskii-type models) in order to describe phenomenologically non-equilibrium physics of exciton/photon/exciton-polariton condensates. To step beyond the description of the kinetic stage of condensate formation, which had been well studied [12–14] and to incorporate the coherent properties of condensate in the evolution equation, a model was proposed by M. Wouters and I. Carusotto [15], describing polariton condensate as a system, coupled to classical reservoir of density n_R :

$$\begin{cases} i\dot{\psi} = \left\{ -\frac{\hbar^2 \nabla^2}{2m} + \frac{i}{2} [R(n_R) - \gamma] + g|\psi|^2 + 2\tilde{g}n_R \right\} \psi, \\ \dot{n}_R = P - \gamma_R n_R - R(n_R) |\psi(\mathbf{r})|^2 + D \nabla^2 n_R. \end{cases} \quad (1)$$

Here P describes incoherent pumping, $R(n_R)$ is an amplification rate of reservoir-condensate scattering, g and \tilde{g} stand for intracondensate and condensate-reservoir particle interaction. Parameters γ_R and γ are decay rates of quasiparticles from reservoir and condensate.

Another approach was developed with gain saturation term introduced directly in the condensate evolution equation:

$$i\hbar\dot{\psi} = \left[-\frac{\hbar^2 \nabla^2}{2m} + g|\psi|^2 + i(\gamma_{\text{eff}} - \Gamma_{\text{eff}}|\psi|^2) \right] \psi. \quad (2)$$

These appeared to be fruitful models, which allowed to describe spontaneous vortex lattice formation [16], pattern formation [17], as well as relaxation oscillations were considered [18].

Moreover, the dissipative term, first used by L.P. Pitaevskii [19] for superfluid He II, was adopted for describing frequency dependent gain due to the polariton-polariton interaction [20]:

$$i\hbar\dot{\psi} = \left[-\frac{\hbar^2 \nabla^2}{2m} + g|\psi|^2 + iP \left(1 - \frac{i\partial_t}{\Omega_{\text{tr}}} \right) + i(\gamma - \Gamma|\psi|^2) \right] \psi. \quad (3)$$

Here, close to the threshold frequency Ω_{tr} the gain efficiency decreases to zero. Using such a model for polariton condensate appeared to be necessary when obtaining its excitation spectrum and describing its superfluid properties [20].

N.A. Asriyan: naasriyan@vniia.ru

Along with studying the model equations, microscopic theories were developed for exciton/exciton polariton systems [21, 22] in order to derive evolution equations *ab initio*.

The approaches listed above quite well describe condensate formation dynamics. However, they mainly focus on markovian evolution, assuming the memory effects not to be significant. This is not, however, a universal approach since in quasiparticle systems one may have comparable quasiparticle lifetime and memory times, which does not allow Markovian description even for large time scales. In this paper we propose a microscopically motivated dynamical equation for condensate formation dynamics in 2D finite-lifetime quasiparticle system, which incorporates non-markovian effects also. It allows to naturally describe the origin of the frequency-dependent gain term as a result of condensate interaction with non-condensed particles. We obtain the mean-field phase diagram for a quasiparticle system and demonstrate that finite lifetime of condensate particles may change the dynamics completely, leading to formation of phase overlap regions on the phase diagram. As a demonstration of real-life application of the equation, we will consider the phase diagram for CdTe microcavity polariton gas.

Being motivated by the discussion of spontaneous symmetry breaking in cold atom condensate by H. T. C. Stoof [23, 24], we use the same theoretical framework: the Schwinger-Keldysh technique in path integral formulation. It provides direct access to the condensate order parameter. In markovian regime this approach has been applied to quasiparticle condensates to describe, for instance, photonic condensate in a dye-filled optical microcavity [25], exciton polariton condensates in quantum wells [21, 22], parametrically pumped polariton systems were also considered [26]. In order to keep the description analytically trackable, we use here a single-level condensate model (e.g. assume uniform condensate in a finite-sized system) in the spirit of pioneering articles [12, 14] dealing with exciton condensation.

We start from defining in section 2 the model Hamiltonian for 2D quasiparticles with pair interaction. Here our goal is to develop a general theory, not considering any particular system. Introducing the necessary parameters, we derive the mean-field dynamical equations for condensate evolution in Section 3. This derivation is followed by a description of a possible simplified approximate expression for equation terms. It leads to a dynamical model which is of the main results of the current paper.

The next section 4 is devoted to discussion of a mean-field phase diagram for a generic quasiparticle system. Possible phases are described followed by a stability analysis. A detailed description of condensation dynamics is presented in section 5.

After a discussion on the advantages and drawbacks

of the model description in section 6, in the last section 7 of the article we present an application of the model to real-life system such as exciton polariton gas in CdTe-HgTe-CdTe microcavity.

2 The model system

We deal with a 2D single-level condensate model of finite-lifetime quasiparticles embedded in a long-living particle reservoir. The system is treated as a 2D bose gas with contact interparticle interaction and leakage from the condensate. The model Hamiltonian for the system described is as follows ($\hat{\psi}_{\mathbf{q}}$ is the quasiparticle annihilation operator with wavevector \mathbf{q} , therefore $\hat{\psi}_0$ corresponds to the condensate mode):

$$\hat{H} = \left(\varepsilon - i\frac{\Gamma}{2} \right) \hat{\psi}_0^\dagger \hat{\psi}_0 + \sum_{\mathbf{q} \neq \mathbf{0}} \varepsilon_{\mathbf{q}} \hat{\psi}_{\mathbf{q}}^\dagger \hat{\psi}_{\mathbf{q}} + g_0 \sum_{\mathbf{q}_1, \mathbf{q}_2, \mathbf{q}'} \hat{\psi}_{\mathbf{q}_1 + \mathbf{q}'}^\dagger \hat{\psi}_{\mathbf{q}_2 - \mathbf{q}'}^\dagger \hat{\psi}_{\mathbf{q}_1} \hat{\psi}_{\mathbf{q}_2} \quad (4)$$

Here $g_0 = \frac{V_0}{2L^2}$ stands for contact interparticle interaction with V_0 being the interaction potential and L^2 denoting the quantization area. ε denotes the possible energy detuning of the condensate level with respect to the reservoir dispersion curve $\varepsilon_{\mathbf{q} \rightarrow 0} = 0$. A decay rate Γ is introduced to describe condensate particle finite lifetime. Hereafter $\hbar = 1$.

The action for this system defined on the Schwinger-Keldysh contour in path integral formulation is as follows:

$$S = \int_c d\tau \left[\bar{\psi}_0 \left\{ i\partial_\tau - \varepsilon + i\frac{\Gamma}{2} \right\} \psi_0 - \sum_{\mathbf{q} \neq \mathbf{0}} \bar{\psi}_{\mathbf{q}} \left\{ i\partial_\tau - \varepsilon_{\mathbf{q}} \right\} \psi_{\mathbf{q}} \right] - g_0 \int_c d\tau \sum_{\mathbf{q}_1, \mathbf{q}_2, \mathbf{q}'} \bar{\psi}_{\mathbf{q}_1 + \mathbf{q}'} \bar{\psi}_{\mathbf{q}_2 - \mathbf{q}'} \psi_{\mathbf{q}_1} \psi_{\mathbf{q}_2}. \quad (5)$$

Our goal is to integrate out the reservoir degrees of freedom to derive an effective action for the condensate. We are going to treat the reservoir in the simplest possible way as a continuously pumped quasi-equilibrium system with stationary surface density n and effective temperature $T = (k_B \beta)^{-1}$. Moreover, we assume the collision broadening for the reservoir to be negligible compared to the effective temperature. When considering the greater/lesser components of the Green's function on the Schwinger-Keldysh contour, this allows to use the following approximation (the spectral function is assumed to be a sharply peaked Lorentzian, see Fig. 1):

$$\frac{iG_{\mathbf{q}}^>(\omega)}{2\pi} = A_{\mathbf{q}}(\omega) [1 + f(\beta\omega)] \rightarrow A_{\mathbf{q}}(\omega) [1 + f(\beta(\zeta_{\mathbf{q}} - \mu))],$$

$$\frac{iG_{\mathbf{q}}^<(\omega)}{2\pi} = A_{\mathbf{q}}(\omega) f(\beta\omega) \rightarrow A_{\mathbf{q}}(\omega) f(\beta(\zeta_{\mathbf{q}} - \mu)). \quad (6)$$

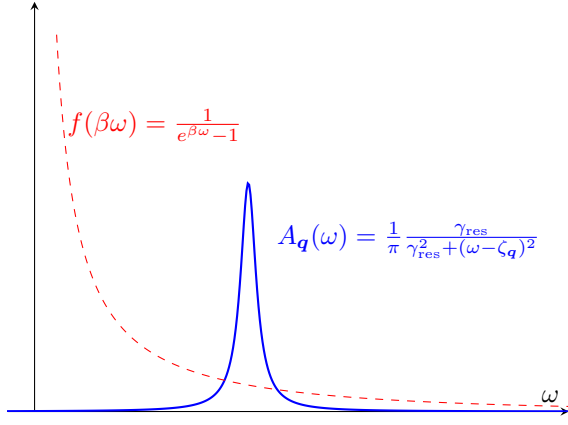


Figure 1: The necessary assumption of “narrow” spectral function.

Here $f(x) = (e^x - 1)^{-1}$, μ stands for the ideal gas chemical potential of the reservoir. From the expressions above, we may combine the casual Green’s function:

$$iG_{\mathbf{q}}^{\text{res}}(t, t') = e^{-\gamma_{\text{res}}|t-t'| - i(\zeta_{\mathbf{q}} - \mu)(t-t')} \times \{\Theta(t, t')(1 + f(\zeta_{\mathbf{q}})) + \Theta(t', t)f(\zeta_{\mathbf{q}})\} \quad (7)$$

with $\gamma_{\text{res}} \rightarrow 0$ and $\zeta_{\mathbf{q}} = \varepsilon_{\mathbf{q}} + \Delta\varepsilon_{\mathbf{q}} - \mu$. Here $\Delta\varepsilon_{\mathbf{q}}$ takes into account the blueshift due to reservoir particle in-

$$S_{\text{eff}}[\phi, \bar{\phi}, \xi, \bar{\xi}] = \int_{\tau_0}^t d\tau \int_{\tau_0}^t d\tau' \bar{\phi} \left[\left\{ i\partial_{\tau} - \varepsilon + i\frac{\Gamma}{2} - \Sigma_0^{\delta} - g_0|\phi|^2 \right\} \delta(\tau, \tau') - \Sigma_0^{-}(\tau, \tau')\theta(t-t') \right] \xi' + \int_{\tau_0}^t d\tau \int_{\tau_0}^t d\tau' \bar{\xi} \left[\left\{ i\partial_{\tau} - \varepsilon + i\frac{\Gamma}{2} - \Sigma_0^{\delta} - g_0|\phi|^2 \right\} \delta(\tau, \tau') - \Sigma_0^{+}(\tau, \tau')\theta(t-t') \right] \phi' - \frac{1}{2} \int_{\tau_0}^t d\tau \int_{\tau_0}^t d\tau' \bar{\xi} \Sigma_0^K(\tau, \tau') \xi' \quad (10)$$

with local (Σ_0^{δ}), retarded (Σ^+), advanced (Σ_0^{-}) and Keldysh (Σ_0^K) components of the self-energy term introduced.

$$\begin{aligned} -\Sigma_{\mathbf{q}}^{\delta}(t, t') &= 2 \text{ (diagram: a filled circle with a clockwise arrow labeled } q_1 \text{)} \\ -\Sigma_{\mathbf{q}}(t, t') &= 8i \text{ (diagram: two circles connected by two horizontal lines, with arrows labeled } q_1 \text{ and } q_2 \text{)} \end{aligned}$$

Figure 2: Time-local term and the contribution to the self-energy term due to interaction with reservoir. Here the filled vertex corresponds to the factor $(-g_0)$, solid lines are reservoir Green’s functions $G_{\mathbf{q}}^{\text{res}}$, given by (7).

To derive the dynamical equation from this type of action, one needs to treat noise terms coupled to the ϕ field dynamics, which leads to a Langevin type equation. In the current paper, we focus on the mean-field dynamics by seeking the stationary phase “classical”

teraction.

3 Deriving dynamical equations

3.1 Effective action

We may integrate out reservoir degrees of freedom in order to obtain an effective action for the condensate mode only (with ψ being the corresponding field), which has the following structure:

$$S^{\text{eff}} = \int_c d\tau \bar{\psi} \left\{ i\partial_{\tau} - \varepsilon_0 + i\frac{\Gamma}{2} - \Sigma_0^{\delta} - g_0|\psi|^2 \right\} \psi - \int_c d\tau \int_c d\tau' \bar{\psi}(\tau) \Sigma_0(\tau, \tau') \psi(\tau'). \quad (8)$$

Here we introduced a self-energy term Σ to describe interaction with reservoir, extracting the time-local contribution $\Sigma^{\delta}(\tau, \tau') = \Sigma^{\delta}\delta(\tau, \tau')$ explicitly, We use the lowest order diagrammatic expressions for these terms as presented on Fig. 2.

After performing the standard Keldysh rotation

$$\psi_{\pm} = \phi \pm \frac{\xi}{2}, \quad (9)$$

the real-time action acquires the following form:

solution in a form:

$$\frac{\delta S_{\text{eff}}}{\delta \phi} = 0 \rightarrow \xi(t) = 0, \quad (11)$$

$$\frac{\delta S_{\text{eff}}}{\delta \xi} = 0 \rightarrow \phi(t) = \phi_c(t). \quad (12)$$

with the latter being a solution of the following equation:

$$i\dot{\phi}_c = \left[\varepsilon - i\frac{\Gamma}{2} + \Sigma_0^{\delta} + g_0|\phi_c|^2 \right] \phi_c(t) + \int_{t_0}^t d\tau \Sigma_0^{+}(t, \tau) \phi_c(\tau). \quad (13)$$

Analysing this equation is the main objective of the current work.

Neglecting the noise term imposes several limitations. Namely, we are not able to describe correctly the initial stages of condensate evolution when fluctuations dominate the dynamics. The approach presented below leads to relevant results in the vicinity

of stationary points, where noise terms are less significant. Incorporating them terms into the theory is left for future investigations.

3.2 Self-energy term

As we see on Fig. 2, the self-energy term besides an evident blueshift contribution

$$\Sigma_{\mathbf{q}}^{\delta} = g_0 \sum_{\mathbf{q}_1} f(\zeta_{\mathbf{q}_1} - \mu) = 2g_0 N^{\text{res}} = V_0 n^{\text{res}} \quad (14)$$

(with N^{res} and n^{res} being the total reservoir occupation and its surface density correspondingly) has a

$$\Sigma_0^+(\tau) = -8ig_0^2 e^{-3\gamma_{\text{res}}\tau} \sum_{\mathbf{q}_1, \mathbf{q}_2} e^{-i(\varepsilon_{\mathbf{q}_1} + \varepsilon_{\mathbf{q}_2} - \varepsilon_{\mathbf{q}_1 + \mathbf{q}_2})t} [f_{\mathbf{q}_1} (1 + f_{\mathbf{q}_1 + \mathbf{q}_2}) f_{\mathbf{q}_2} - (1 + f_{\mathbf{q}_1}) f_{\mathbf{q}_1 + \mathbf{q}_2} (1 + f_{\mathbf{q}_2})] \Theta(\tau). \quad (16)$$

Considering $\gamma_{\text{res}} \rightarrow 0$ as well as taking advantage of the Bose-Einstein distribution property $1 + f(\omega) = e^{\omega} f(\omega)$, we obtain the following expression for the imaginary part of the retarded component (here $f_{\mathbf{q}} = f[\beta(\varepsilon_{\mathbf{q}} - \mu)]$):

$$\Im[\Sigma_0^+(\omega)] = -8g_0^2 \left[e^{\beta(\omega - \mu)} - 1 \right] \sum_{\mathbf{q}_1, \mathbf{q}_2} f_{\mathbf{q}_1} (1 + f_{\mathbf{q}_1 + \mathbf{q}_2}) f_{\mathbf{q}_2} \delta(\omega + \varepsilon_{\mathbf{q}_1 + \mathbf{q}_2} - \varepsilon_{\mathbf{q}_1} - \varepsilon_{\mathbf{q}_2}). \quad (17)$$

With dimensionless sum isolated as follows:

$$\Im[\Sigma_0^+(\omega)] = \frac{V_0^2}{(2\pi)^3 \lambda_{dB}^4} I(\omega) \quad (18)$$

with $\lambda_{dB} = \frac{\hbar}{\sqrt{2mT}}$ being the thermal de-Broglie wavelength. Hereafter $\beta = 1$, which means all the energies are measured in units of kT .

One may evaluate $I(\omega)$ numerically, considering quadratic dispersion relation. Moreover, asymptotic behaviour may be studied analytically (see Appendix A to find calculations for arbitrary momentum \mathbf{q}). All the information is summarized on Fig. 3.

When discussing the $\omega \rightarrow \infty$ asymptotics, we note that $I(\omega) = \text{const}$ does not vanish. This is due to the contribution of the following process: a virtual particle with $q = 0$ and $\varepsilon = \omega$ scatters on a reservoir particle with $q \approx 0$, $\varepsilon_{\mathbf{q}} \approx 0$. As a result, they are both in the reservoir with momenta $\mathbf{q}_1 = -\mathbf{q}_2$ and energies $\varepsilon_{\mathbf{q}_1} = \varepsilon_{\mathbf{q}_2} = \frac{\omega}{2}$. The amplitude of this process does not decrease with growing ω . This is a consequence of the contact interaction model. If we consider some finite interaction radius, *i.e.*, introduce a transfer momentum cut-off, $I(\omega)$ will tend to zero with growing ω because of growing transferred momentum $q \sim \sqrt{\omega}$ during the scattering process. This is schematically demonstrated by a dash-dotted red line on Fig. 3. The exact behaviour depends, of course, on the interparticle interaction potential.

term due to interparticle interaction (here $\tau = t - t'$):

$$\Sigma_{\mathbf{q}}(\tau) = -8g_0^2 \sum_{\mathbf{q}_1, \mathbf{q}_2} G_{\mathbf{q}_1}^{\text{res}}(\tau) G_{\mathbf{q}_1 + \mathbf{q}_2 - \mathbf{q}}^{\text{res}}(-\tau) G_{\mathbf{q}_2}^{\text{res}}(\tau). \quad (15)$$

Note that the term $\Sigma_{\mathbf{q}}^{\delta}$ is independent of \mathbf{q} , therefore reservoir states are shifted by the same amount and the energy offset ε is not affected by Σ^{δ} . In fact, by this we use the Hartree-Fock approximation for the reservoir (for contact interaction direct and exchange terms give the same contribution, that's why we have a factor of 2 when expressing Σ^{δ} on fig. 2).

For the retarded component, one obtains the following expression by setting $\mathbf{q} = 0$ (partly following [22] by two of us):

Using this numerical result for further calculations is quite involved. We will further use an approximation

$$\Im[\Sigma_0^+(\omega)] = -\Lambda^+ \frac{\omega - \mu}{\gamma^2 + \omega^2}, \quad (19)$$

which captures the double-peaked shape of the curve as well as reproduces the x -intercept correctly, which appears to be important to describe condensate effective chemical potential equilibration. Here, Λ^+ and γ may be treated as fitting parameters.

Of course, the model curve cannot reproduce the real one exactly. As we will discuss in section 7, when searching the best fit parameters, it's worth better fitting the left peak at the cost of not reproducing the high-frequency behaviour as demonstrated on Fig. 3.

The retarded self-energy term is analytic in the upper half plane in frequency domain due to causality, therefore its real and imaginary part are related by the Kramers-Kronig relations, and we may seek an approximation for the function using its imaginary part only. Therefore:

$$\Sigma_0^+(\omega) = -\Lambda^+ \frac{\gamma^2 + \omega\mu}{\gamma^2 + \omega^2} - i\Lambda^+ \frac{\omega - \mu}{\gamma^2 + \omega^2}. \quad (20)$$

In time domain this function is as follows (note that time is measured in units of $1/kT$):

$$\Sigma_0^+(t) = -\Lambda^+ \left(1 - i\frac{\mu}{\gamma} \right) e^{-\gamma t} \Theta(t). \quad (21)$$

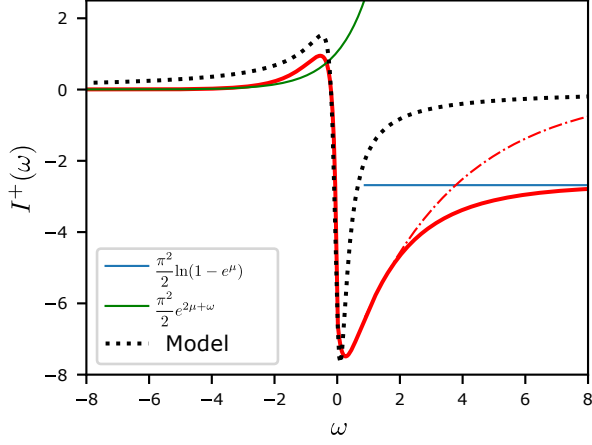


Figure 3: Frequency dependence of the retarded self-energy term component $I(\omega)$ (red solid line) with asymptotics given. The dash-dotted line qualitatively demonstrates how the curve will be modified for finite-range interaction. Here for illustration $\mu = -0.2$ is chosen.

$$\begin{aligned} \partial_t \rho &= -\Gamma \rho - 2\sqrt{\rho} \Lambda^+ \int_0^t dt' e^{-\gamma(t-t')} \sqrt{\rho'} \sin[\theta - \theta'] + 2\frac{\mu}{\gamma} \sqrt{\rho} \Lambda^+ \int_0^t dt' e^{-\gamma(t-t')} \sqrt{\rho'} \cos[\theta - \theta'], \\ \rho \partial_t \theta &= (\varepsilon + g\rho) \rho - \sqrt{\rho} \Lambda^+ \int_0^t dt' e^{-\gamma(t-t')} \sqrt{\rho'} \cos[\theta - \theta'] - \frac{\mu}{\gamma} \sqrt{\rho} \Lambda^+ \int_0^t dt' e^{-\gamma(t-t')} \sqrt{\rho'} \sin[\theta - \theta'], \end{aligned} \quad (23)$$

which leads to the ODE system after differentiating and excluding integral terms:

$$\begin{aligned} \dot{\rho} &= -\Gamma \dot{\rho} + \left(\frac{\dot{\rho}}{2\rho} - \gamma \right) (\dot{\rho} + \Gamma \rho) \\ &\quad + 2\frac{\Lambda^+ \mu}{\gamma} \rho + 2\rho \dot{\theta} (\dot{\theta} - \varepsilon - g\rho), \end{aligned} \quad (24)$$

$$\begin{aligned} \dot{\rho} \dot{\theta} + \rho \ddot{\theta} &= (\varepsilon + 2g\rho) \dot{\rho} + \left(\frac{\dot{\rho}}{2} - \gamma \rho \right) \\ &\quad \times (\dot{\theta} - \varepsilon - g\rho) - \frac{\dot{\theta}}{2} (\dot{\rho} + \Gamma \rho) - \Lambda^+. \end{aligned} \quad (25)$$

To get rid of negative power terms in ρ , we may now use $\rho(t) = e^{r(t)}$ substitution in order to obtain the following autonomous ODE system:

$$\begin{aligned} \ddot{r} &= -\left(\frac{\Gamma}{2} + \gamma \right) \dot{r} - \frac{\dot{r}^2}{2} + \left(2\frac{\Lambda^+ \mu}{\gamma} - \gamma \Gamma \right) + 2\dot{\theta} (\dot{\theta} - \varepsilon - g e^r), \\ \ddot{\theta} &= (\varepsilon + 2g e^r) \dot{r} - \frac{3}{2} \dot{r} \dot{\theta} + \left(\frac{\dot{r}}{2} - \gamma \right) (\dot{\theta} - \varepsilon - g e^r) - \frac{\Gamma \dot{\theta}}{2} - \Lambda^+. \end{aligned} \quad (26)$$

By introducing $V = \dot{r}$ and $\nu = \dot{\theta}$ as new variables, we may formulate the dynamical equation as a first order

4 Mean-field phase diagram

4.1 Reduction to an ODE system

Using (21), we may write down the dimensionless dynamical equation as follows:

$$\begin{aligned} i\partial_t \phi_c &= \left(\varepsilon + g|\phi_c|^2 - i\frac{\Gamma}{2} \right) \phi_c \\ &\quad - \Lambda^+ \left(1 - i\frac{\mu}{\gamma} \right) \int_0^t e^{-\gamma(t-t')} \phi_c(t') dt' \end{aligned} \quad (22)$$

The advantage provided by using an exponential kernel is the possibility to simplify the dynamical equation (22). To do that, one may consider it along with its time derivative in order to exclude the memory term. Namely, the Madelung transformation $\phi_c(t) = \sqrt{\rho(t)} e^{-i\theta(t)}$ is performed (time arguments are omitted, $\rho' \equiv \rho(t')$, $\theta' \equiv \theta(t')$):

ODE system:

$$\begin{aligned} \dot{V} &= \left(2\frac{\Lambda^+ \mu}{\gamma} - \gamma \Gamma \right) + \left(\frac{\Gamma}{2} + \gamma \right) V - \frac{V^2}{2} + 2\nu(\nu - \varepsilon - g e^r), \\ \dot{\nu} &= (\varepsilon + 2g e^r) V - \frac{3V\nu}{2} + \left(\frac{V}{2} - \gamma \right) (\nu - \varepsilon - g e^r) - \frac{\Gamma \nu}{2} - \Lambda^+, \\ \dot{r} &= V. \end{aligned} \quad (27)$$

To derive initial conditions, one may set $t = 0$ in (23):

$$\begin{cases} \partial_t \rho(0) = -\Gamma \rho, \\ \rho \partial_t \theta(0) = (\varepsilon + g\rho) \rho. \end{cases} \quad (28)$$

This leads to $\nu(0) = \varepsilon + g e^r$ and $V(0) = -\Gamma$. Note that these expressions are due to assuming the condensate and reservoir being in contact from $t = 0$ exactly. In real system the initial evolution stages may be more complicated, which, however, does not change the asymptotic behaviour of the system.

4.2 Stationary points

Here, we seek stationary points of the ODE system (27) by setting $\dot{V} = \dot{r} = \dot{\nu} = 0$:

$$\begin{cases} 2\nu(\nu - \varepsilon - g\rho) = -2\frac{\mu}{\gamma} \Lambda^+ + \gamma \Gamma, \\ \gamma(\nu - \varepsilon - g\rho) + \frac{1}{2} \Gamma \nu = -\Lambda^+. \end{cases} \quad (29)$$

We readily solve these equations to obtain:

$$\nu_{\pm} = \frac{-\Lambda^+ \pm \sqrt{D}}{\Gamma}, \quad (30)$$

$$\rho_{\pm} = \frac{1}{g} \left[-\varepsilon + \Lambda^+ \left(\frac{1}{2\gamma} - \frac{1}{\Gamma} \right) \pm \left(\frac{1}{\Gamma} + \frac{1}{2\gamma} \right) \sqrt{D} \right] \quad (31)$$

with

$$D = -\gamma^2 \Gamma^2 + (\Lambda^+)^2 + 2\Gamma \Lambda^+ \mu. \quad (32)$$

For stability analysis of these stationary points, one may consider the linear expansion and obtain the corresponding eigenvalues (see Appendix B). The “upper” solution with “+” sign appears to be stable and the “lower” one – unstable.

4.3 Decaying solution

Dealing with a constrained quantity $\rho \geq 0$, we should consider one more equilibration scenario with $\rho \rightarrow 0$. We may seek the decaying solution in a form $\dot{r} = 0$, $\dot{r} = \kappa$, $\dot{\theta} = \Omega = \text{const}$. With small ρ being neglected, this leads to the following characteristic equations:

$$\begin{cases} \frac{\kappa^2}{2} = -\left(\frac{\Gamma}{2} + \gamma\right) \kappa + \left(2\frac{\mu}{\gamma}\Lambda^+ - \gamma\Gamma\right) + 2\Omega(\Omega - \varepsilon) \\ 0 = -\frac{3}{2}\kappa\Omega + \varepsilon\kappa + \left(\frac{\kappa}{2} - \gamma\right)(\Omega - \varepsilon) - \frac{1}{2}\Gamma\Omega - \Lambda^+ \end{cases} \quad (33)$$

As derived in Appendix B, there are two eigenmodes with $\kappa < 0$ (*i.e.*, the decaying solution is stable) whenever $\rho_+ \rho_- \geq 0$ or $D < 0$. Stated otherwise, the decaying solution is stable if there are either no stationary points or both of them are present simultaneously.

4.4 Phase diagram

From the discussion above, we infer that there are two possible equilibration scenarios. The one is reaching a stationary solution ρ_+ and the other is a decaying solution. In physical terms, the first one corresponds to condensate formation (with non-zero ϕ being the corresponding order parameter) and the second one describes the normal phase.

Using the results of the stability analysis, we may summarize them on a phase diagram presented on Fig. 4 on (Λ^+, Γ) plane (Λ^+ physically corresponds to condensate-reservoir interaction “strength”, Γ is the decay intensity of condensate particles). The remaining parameters γ and μ are fixed.

On this figure, the condensate exists whenever $\rho_+ > 0$ (which implies $D > 0$). The more strict condition of these two ($\rho_+ > 0$ and $D > 0$) defines the condensate stability boundary.

The decaying solution is stable in the three cases listed below:

1. For regions with $D < 0$. Here no stationary points exists, decay is the only asymptotic scenario. This is the “Normal phase” region of the diagram, below the dashed straight line.

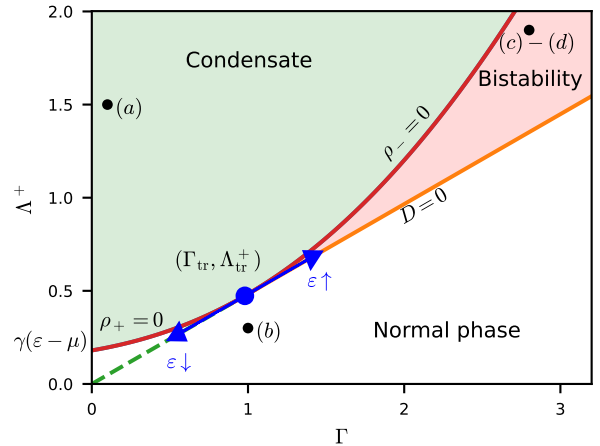


Figure 4: Phase diagram for the system under consideration. The blue dot denotes the “triple” point of coexistence of all the three phases. The arrows indicate how does this point move with varying ε . Here for demonstration $\gamma = 0.2, g = 1, \mu = -0.2, \varepsilon = 0.7$. For each of the black dots (a)-(d) there is an evolution graph presented on Fig. 5.

2. When $D > 0$ but $\rho_- < 0$ as well as $\rho_+ < 0$. There are also no physically relevant stationary points here, this is another part of the “Normal phase” region, which is in the left bottom corner of the diagram, below the dashed line. Note that for low enough, ε this region disappears (*e.g.* on Fig. 6).
3. For $D > 0$, $\rho_+ > 0$ and $\rho_- > 0$. Here both the decaying solution and one of the stationary points are stable. This is the “Bistability” region on the phase diagram bounded by $D = 0$ and $\rho_- = 0$ lines (note that $\rho_- < \rho_+$, that’s why it is $\rho_- < 0$ which makes stability criterion $\rho_- \rho_+ > 0$ invalid). This is kind of an overlap of “Normal phase” and “Condensate” regions of the phase diagram.

The equations of the phase boundaries are presented near the corresponding lines.

There is kind of a triple point on the phase diagram where all the three solutions coexist with $\rho_{\pm} \rightarrow 0$. Its position is given by

$$\begin{cases} \Gamma_{\text{tr}} = 2\gamma \left(1 + \frac{\varepsilon}{\sqrt{\gamma^2 + \mu^2 - \mu}} \right), \\ \Lambda_{\text{tr}}^+ = 2\gamma \left(\sqrt{\gamma^2 + \mu^2 - \mu} + \varepsilon \right) \end{cases} \quad (34)$$

and regardless of the detuning, ε it is located on the straight line $\Lambda^+ = \left(\sqrt{\gamma^2 + \mu^2 - \mu} \right) \Gamma$ (as indicated by blue arrows on the dashed line on fig. 4).

Note that for $\Gamma \rightarrow 0$, only the “upper” stationary

point exists. It is given by:

$$\nu = \mu, \quad (35)$$

$$\rho = \frac{1}{g} \left[\mu - \varepsilon + \frac{\Lambda^+}{\gamma} \right]. \quad (36)$$

The effective chemical potential ν of the condensate becomes equal to the one of the particle reservoir, as one could expect for atomic gas of long-living particles. The condensation threshold may be identified at $\rho \rightarrow 0$ (see the y-intercept on Fig. 4):

$$\Lambda^+ = \gamma(\varepsilon - \mu). \quad (37)$$

Since Λ^+ itself is not an independent quantity but depends on density and temperature, this equation may be treated as a one defining the critical effective temperature T_c^{eff} . When increasing condensate decay rate, this temperature gets shifted. A demonstration of critical temperature evaluation will be presented in sec. 7.

5 Dynamics

5.1 Evolution in different regimes

In the two of the three phases described, condensate formation is possible. In the ‘‘Condensate’’ phase there is a single stationary point present which attracts all the ODE solutions regardless of the initial conditions as demonstrated on Fig. 5 (a).

In contrast, in the ‘‘Normal phase’’ region all the solutions are attracted towards $\rho = 0$ with $\dot{\theta}$ approaching ν_∞ , which corresponds to the slower decaying eigenmode as illustrated on Fig 5 (b) (see Appendix B for details).

In the bistability regime an unstable stationary point appears which repels the occupation to either $\rho = 0$ or the stable point as illustrated on Fig. 5 (c)-(d). Note that on Fig. 5 (c) the upper stationary point also exists at a higher occupation.

One may infer, studying the evolution in the bistable regime, that higher initial occupations are attracted to the stationary point (condensate formation takes place as on Fig. 5 (d)) and lower ones decay to zero as presented on Fig. 5 (c). However, it is not always the case, since for some parameters even for large ρ the line of initial condition $\nu = \varepsilon + g\rho$ does not intersect the attraction basin of the stable point.

5.2 Condensate formation. Relaxation oscillations

On fig 5 (a) one may see oscillations when approaching equilibrium. Though, such type of relaxation oscillations are not a general feature of the system.

As it is shown in details in Appendix B, the eigenmode expansion of $\phi(t)$ close to stationary state consists of terms $e^{\kappa_0 t}$, $e^{(\kappa_1 \pm i\Omega)t}$. We expect significant

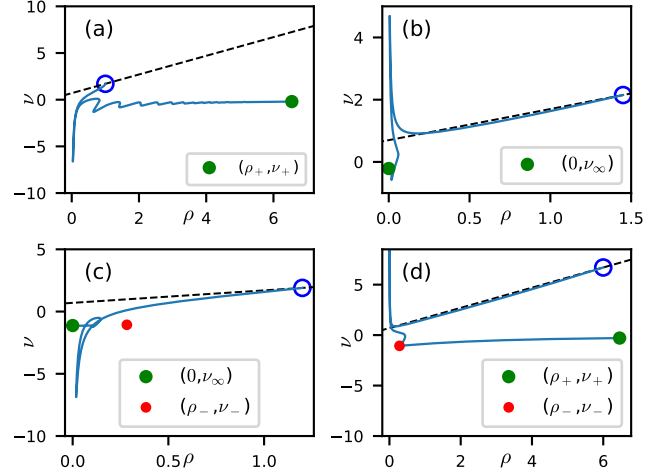


Figure 5: Evolution illustrated for (a) ‘‘Condensate’’ phase; (b) ‘‘Normal phase’’; (c)-(d) ‘‘Bistability’’ phase for two initial occupations. The letters correspond to points on Fig. 4. The dashed line restricts the initial conditions by $\nu = \varepsilon + g\rho$ as given by (28). The hollow circle indicates the initial occupation chosen.

asymptotic density oscillations similar to the ones described in the scope of a different model in [18], when $\kappa_0 < \kappa_1$ (note that both are negative) in order for the oscillatory terms to dominate at late times. This regime is illustrated on Fig. 7 (a)-(c). In contrast, for $\kappa_0 > \kappa_1$ at late times condensate occupation monotonously approaches stationary value as shown on Fig. 7 (d)-(f).

Relaxation oscillations are present for low enough ε , the typical phase diagram for this regime is presented on Fig. 6.

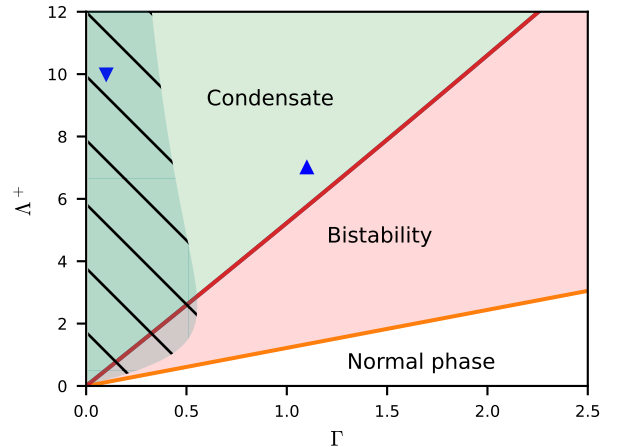


Figure 6: Phase diagram for low enough ε . In the hatched region $\kappa_0 < \kappa_1$, asymptotic dynamics is oscillatory. Here for demonstration $\gamma = 1$, $g = 1$, $\mu = -0.2$, $\varepsilon = -10$.

Of course, the oscillations may be observable outside the hatched region of the phase diagram also. However, at late times, they are replaced by monotonous exponential approach to the stationary

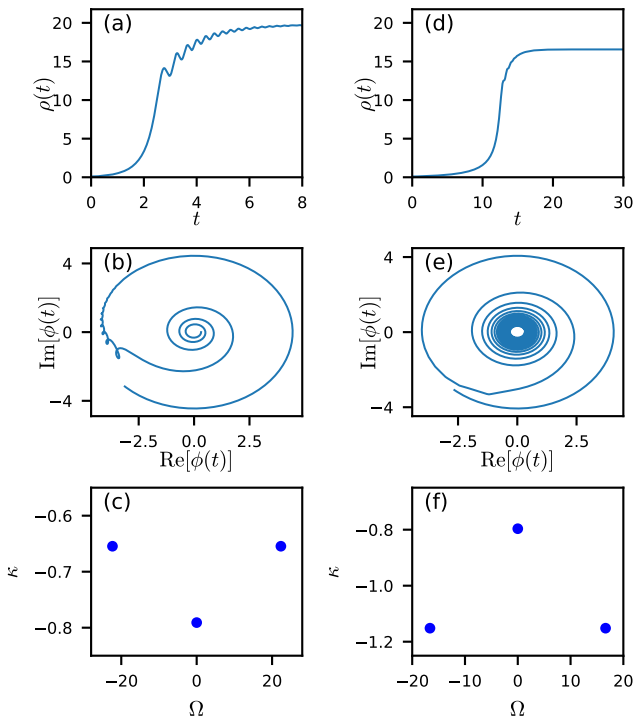


Figure 7: (a), (b) Relaxation oscillations at $\Gamma = 0.1$, $\Lambda^+ = 10$. (c) Eigenmodes for this case. These plots correspond to \blacktriangledown on Fig. 6. (d), (e) Monotonous asymptotics for $\Gamma = 1.1$, $\Lambda^+ = 7$. (f) Eigenmodes for this case. These plots correspond to \blacktriangle on Fig. 6.

state.

5.3 Bifurcation scheme

In order to draw several physical predictions in the bistable region, we study here the bifurcation diagram of the ODE system. It is presented schematically on Fig. 8 for fixed Γ , μ , g and ε . It may be treated as a cross-section of the phase diagram Fig. 4 by a vertical line passing to the right of the “triple point”.

We readily observe the bistable region where there are two stable branches. Along with the repelling behaviour of the lower stationary point, illustrated on Fig. 5 (c)-(d), we expect two physical effects in this region.

Foremost, when condensate is formed in the bistability region, hysteresis is possible when changing the Λ^+ by varying the quasiparticle density. This is illustrated by a cycle of violet arrows on Fig. 8.

The second prediction is related to condensate formation dynamics. One should note that initial conditions for ϕ_c cannot be defined precisely, at least due to uncertainty relation. We may set up the initial distribution only. This makes condensate formation a probabilistic process. In any particular realization with all the other parameters being the same, the system may end up either in normal or in condensed phase.

Detailed study of both these effects is beyond the scope of the mean-field analysis, fluctuations should

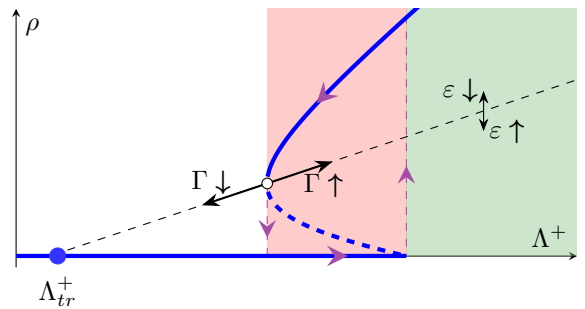


Figure 8: Bifurcation diagram for the bistable region of the phase diagram. The stable solution branches are drawn as solid curves, for the unstable one a thick dashed curve is used. The bifurcation point is pictured in white. Arrows indicate its movement along the dashed line with Γ being changed. The double arrow on the right indicates how does the line move with ε being varied.

be systematically treated.

6 Discussion

6.1 Alternative treatment. Origin of phases

The integro-differential equation (13) itself may provide some useful qualitative understanding even without converting it to an ODE system. Namely, considering a stationary solution in a form $\phi_c = \sqrt{\rho}e^{-i\nu t}$ (assuming non-zero ρ and $\nu = \text{const}$), we may derive the following pair of equations:

$$\begin{cases} \nu = [\varepsilon_0 + \Sigma^\delta + g\rho] + \Re[\Sigma_0^+(\nu)], \\ \Im[\Sigma_0^+(\nu)] - \frac{\Gamma}{2} = 0. \end{cases} \quad (38)$$

The first of them provides a relation for the self-consistent effective chemical potential ν of the condensate. The second one describes particle flux saturation. Obviously, we should impose a constraint $g\rho \geq 0$, therefore, the necessary condition for condensation is existence of a non-empty set of zeros ν^* of the imaginary part $\Im[\Sigma_0^+(\nu)]$, which satisfy the condition $\Re[\Sigma^+(\nu^*)] \leq \nu^* - \varepsilon_0 - \Sigma^\delta$. This condition may be considered as another version of the condensate formation criterion described by H.T.C. Stoof in [23] when describing spontaneous symmetry breaking in cold atomic gas.

These general statements may be illustrated with the use of the model expression for the self-energy term. The equation (22) leads to

$$\begin{cases} \nu = \varepsilon + g\rho - \frac{\Lambda^+}{\gamma} \frac{\gamma^2 + \nu\mu}{\gamma^2 + \nu^2}, \\ \frac{\Gamma}{2} = \Lambda^+ \frac{\mu - \nu}{\gamma^2 + \nu^2}. \end{cases} \quad (39)$$

The stationary points (ν_\pm, ρ_\pm) may be obtained from the graphical representation of the equation system (39) below on Fig. 9.

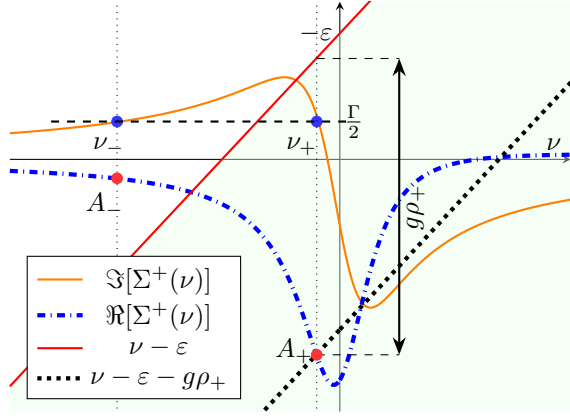


Figure 9: Solving graphically the equation system (39)

One may identify two intersection points of $\Im[\Sigma^+(\nu)]$ with $\frac{\Gamma}{2}$ on Fig. 9 as the ones, corresponding to the two stationary points (30). By solving the first equation of the system with ν_{\pm} with respect to ρ , we find stationary occupation numbers ρ_{\pm} , which are physically relevant if $\rho \geq 0$. Graphically $\rho_{\pm} > 0$ when the corresponding points A_{\pm} with coordinates $(\nu_{\pm}, \Re[\Sigma^+(\nu_{\pm})])$ are in the shaded region below the line $\nu - \varepsilon$. For instance, on Fig. 9 only one stationary point A_+ is in the shaded region, which corresponds to the "Condensate" phase.

This qualitative discussion provides an illustration to the claim from section 2 about focusing on the left peak when fitting the $\Im[\Sigma(\omega)]$ curve, since it defines the stationary points. This is by no means a solid statement, since the real part of the self energy may be significantly modified even in the vicinity of $\omega = 0$ along with changing the high-frequency behaviour of the imaginary part. It means that our model is incapable of describing fine effects due to the exact form of the interparticle interaction (which defines mostly how exactly does the $\Im[\Sigma(\omega)]$ decay at high frequencies). It is suitable for qualitative description only.

However, for an arbitrary $\Sigma^+(\omega)$ one can apply the same graphical procedure and seek solutions in the shaded region where $\nu - \varepsilon \geq \Re[\Sigma(\nu)]$. This approach allows not only equilibrating the occupation $\rho = |\phi|^2$ of the condensate, but also describing the spontaneous symmetry breaking and stationary phase dynamics.

6.2 Reservoir particle interaction

As one may infer from equation system (38), the condensate formation is crucially dependent on the form of $\Re[\Sigma_0^+(\omega)]$. Moreover, since reservoir levels may be shifted also, the relative offset $\Re[\Sigma_0^+(\omega) - \Sigma_{\mathbf{q}}^+(\omega)]$ with respect to reservoir states with non-zero \mathbf{q} is relevant. Taking this into account will change the quantitative predictions of the theory. However, as demonstrated in Appendix A, the qualitative behaviour of $\Sigma^+(\mathbf{q})$ is independent of q , the double-peaked shape remains the same as well as $\Sigma_{\mathbf{q}}^+(\mu) = 0$ for arbitrary \mathbf{q} . That's why a more thorough treatment (the one similar to

what is done for 3D cold atom gas in Ref. [28]) will not change qualitative predictions of the model.

6.3 Markovian limit

We may now show how the model equation (22) is related to the Markovian Gross-Pitaevski model (2) (for uniform system since we deal with a single-level condensate). To do that, one should consider the particle flux dependence on the condensate occupation number. As discussed above, using an ansatz $\phi = \sqrt{\rho}e^{-i\nu t}$, one may derive the equation pair (39) from (22). By expanding near the stable stationary point (ν_+, ρ_+) , we express the particle flux as follows:

$$d_t |\phi|^2 = \frac{2\Lambda^+ g}{\gamma^2 + \nu_+^2 + \frac{\Lambda^+}{\gamma} \mu} (\rho^+ - |\phi|^2). \quad (40)$$

Note that (2) leads to

$$d_t |\phi|^2 = 2(\gamma_{\text{eff}} - \Gamma_{\text{eff}} |\phi|^2). \quad (41)$$

Therefore, close to the stable point the first model reproduces the second with

$$\gamma_{\text{eff}} = \frac{\Lambda^+ g \rho_+}{\gamma^2 + \nu_+^2 + \frac{\Lambda^+}{\gamma} \mu}, \quad (42)$$

$$\Gamma_{\text{eff}} = \frac{\Lambda^+ g}{\gamma^2 + \nu_+^2 + \frac{\Lambda^+}{\gamma} \mu}. \quad (43)$$

However, note that in contrast to (2), the model approach developed here with an exponential memory kernel describes how the reservoir imposes not only the occupation but the condensate effective chemical potential also. This is due to frequency dependent gain, which is described by the frequency dependence of the memory kernel. Though, there were proposed time-local modifications of the Gross-Pitaevski equation (*e.g.*, [20]), which describe frequency-dependent gain, considering explicitly the memory kernel even in a model form allows dealing with non-markovian effects.

This is crucial for describing condensate formation and its phase dynamics. That's what allows us to identify the phase boundaries.

7 Demonstration

Generally one may consider lower polaritons with dispersion

$$E_{\text{LP}}(k) = \frac{k^2}{4} \left[\frac{1}{m_{\text{ph}}} + \frac{1}{m_{\text{ex}}} \right] - \frac{1}{2} \sqrt{\left(\frac{k^2}{2} \left[\frac{1}{m_{\text{ph}}} - \frac{1}{m_{\text{ex}}} \right] + \Delta \right)^2 + 4\Omega^2} \quad (44)$$

Here Ω is the Rabi splitting, m_{ph} and m_{ex} stand for photon and exciton masses respectively, Δ is the photon dispersion detuning with respect to the excitonic

one. It is given as follows (E_g is the semiconductor gap, $E_b < 0$ is the exciton binding energy):

$$\Delta = \frac{hc}{2D} - E_g - E_b \quad (45)$$

with D being here the microcavity width. Condensate is mainly localized at the minimum, and the reservoir particles occupy the “flat” part of the spectrum. Therefore, we may argue that the condensate offset is given by

$$\varepsilon = \frac{\Delta}{2} - \sqrt{\left(\frac{\Delta}{2}\right)^2 + \Omega^2}, \quad (46)$$

which is negative regardless of the sign of Δ .

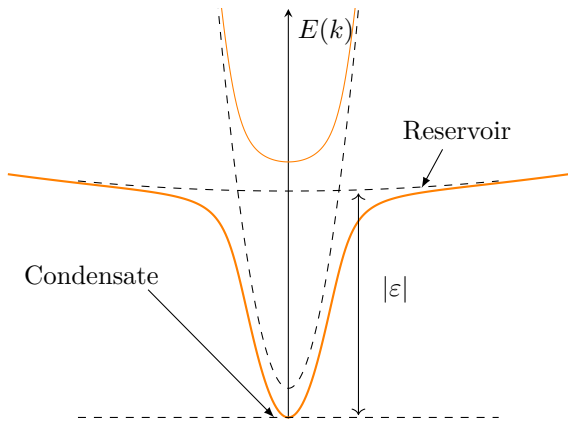


Figure 10: Polariton dispersion. For the lower polariton branch, the energy detuning ε of the condensate with respect to the reservoir is indicated.

When describing polariton-polariton interaction, we need to take into account Hopfield coefficients. It's usually reasonable to consider reservoir particles as having an excitonic component $|X_{\text{res}}|^2 \approx 1$ (being dominantly excitonic).

Since interpolariton interaction is mainly due to the excitonic component, we may use a model Hamiltonian of the following form:

$$\begin{aligned} \hat{H} = & \left(\varepsilon - i\frac{\Gamma}{2} \right) \hat{\psi}_0^\dagger \hat{\psi}_0 + \sum_{\mathbf{q} \neq 0} \varepsilon_{\mathbf{q}} \hat{\psi}_{\mathbf{q}}^\dagger \hat{\psi}_{\mathbf{q}} + g_0 |X_0|^4 \hat{\psi}_0^\dagger \hat{\psi}_0^\dagger \hat{\psi}_0 \hat{\psi}_0 \\ & + g_0 |X_0|^2 \sum_{\mathbf{q}' \neq 0} \left[\hat{\psi}_{\mathbf{q}'}^\dagger \hat{\psi}_{-\mathbf{q}'}^\dagger \hat{\psi}_0^2 + 4 \hat{\psi}_{\mathbf{q}'}^\dagger \hat{\psi}_0^\dagger \hat{\psi}_0 \hat{\psi}_{\mathbf{q}'} + (\hat{\psi}_0^\dagger)^2 \hat{\psi}_{\mathbf{q}'} \hat{\psi}_{-\mathbf{q}'} \right] \\ & + 2g_0 |X_0| \sum_{\mathbf{q}_1, \mathbf{q}_2 \neq 0} \left[\hat{\psi}_0^\dagger \hat{\psi}_{\mathbf{q}_1 + \mathbf{q}_2}^\dagger \hat{\psi}_{\mathbf{q}_1} \hat{\psi}_{\mathbf{q}_2} + \hat{\psi}_{\mathbf{q}_1}^\dagger \hat{\psi}_{\mathbf{q}_2}^\dagger \hat{\psi}_{\mathbf{q}_1 + \mathbf{q}_2} \hat{\psi}_0 \right] \\ & + g_0 \sum_{\mathbf{q}_1, \mathbf{q}_2 \neq 0} \hat{\psi}_{\mathbf{q}_1 + \mathbf{q}_2}^\dagger \hat{\psi}_{\mathbf{q}_2 - \mathbf{q}_1}^\dagger \hat{\psi}_{\mathbf{q}_1} \hat{\psi}_{\mathbf{q}_2}. \end{aligned} \quad (47)$$

This leads to an additional factor of $|X_0|^2$ for Σ^+ . Moreover, blueshifts for the condensate and the reservoir are different now and we need to renormalize the offset energy as follows:

$$\tilde{\varepsilon} = \frac{\Delta}{2} - \sqrt{\left(\frac{\Delta}{2}\right)^2 + \Omega^2} + 2(|X_0|^2 - 1)g_0 N^{\text{res}}. \quad (48)$$

As a real-life example, we may treat in this fashion a polariton gas in CdTe-HgTe-CdTe microcavities. The necessary parameters are $\Omega = 26$ meV, $m_{\text{exc}} = 0.69$ meV, $\Gamma = 1$ meV and the detuning will be considered to be zero $\Delta = 0$, leading to $\varepsilon = -\frac{\Omega}{2}$ [8].

For each value of the dimensionless chemical potential $\beta\mu$ we may fit the numerically evaluated $\Im[\Sigma^+(\omega)]$ by a model expression (19) to find the corresponding parameters Λ^+ and γ as functions of density and temperature. When doing so, we approximate the left peak as described in sec. 3 B.

This allows to numerically solve further the equations $D = 0$, $\rho_{\pm} = 0$ (which define the phase boundaries as illustrated on Fig. 4).

The phase diagram for this system in terms of physically relevant density and effective temperature is presented on Fig. 11 below.

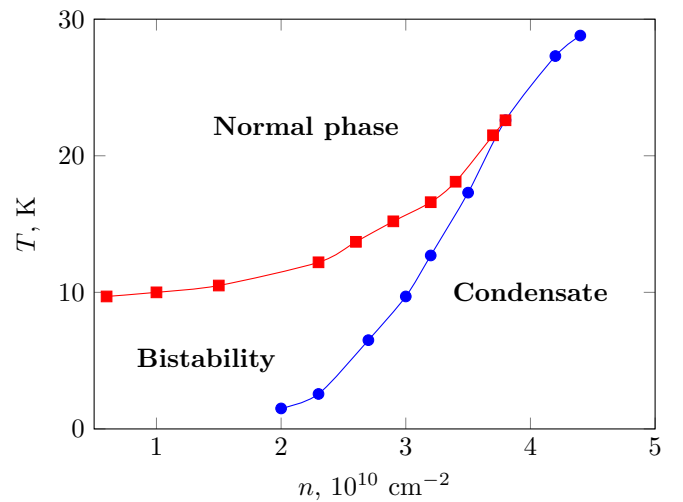


Figure 11: CdTe—HgTe—CdTe microcavity exciton polariton phase diagram

It shows how the model phase diagram on Fig. 4 is mapped on density-temperature plane and allows to localize all the three phases.

8 Conclusion

In this paper we considered a model for describing quasiparticle condensate as an open system embedded in a quasi-equilibrium reservoir. The corresponding open-dissipative Gross-Pitaevski type equation for the condensate has an integral memory term due to the influence of the reservoir. We proposed a simplification, which allows treating the complex integro-differential dynamical equation as an autonomous ODE system. Dealing with stationary solutions of this system, we described a phase diagram predicting the existence of a bistable phase. Several dynamical effects were described, including relaxation oscillations, hysteresis, etc.

To demonstrate the real-life applicability of the model, we considered a polariton gas in CdTe microcavity deriving a phase diagram for this model and localizing the regions of the condensed/normal phases of the system. Though not claiming an agreement with experiment, we expect the form of the phase diagram, in particular the existence of the bistable region, to be a general feature of condensates in quasiparticle systems with finite lifetime.

We see the main advantage of the proposed dynamical equation being its ability to naturally describe frequency-dependent gain and describe correct equilibrium behaviour (in sense of aligning condensate and reservoir chemical potentials) in finite-lifetime limit.

We expect the approach presented here with the structure of the memory kernel proposed to be useful for describing not only the mean field stationary states, but also dynamical, statistical properties far from equilibration. This requires incorporating fluctuations in the model. Doing so and considering coherence build-up in the condensate is a subject of future work.

9 Acknowledgements

N.A.A and Yu.E.L. acknowledge financial support from the Russian Foundation for Basic Research (Grant No 20-02-00410).

A Evaluating the self-energy term

We start the discussion here using an expression from the main text (note that this expression is dimensionless, $\beta = 1$ is considered):

$$\Im[\Sigma_{\mathbf{q}}^+(\omega)] = -8g_0^2 [e^{\omega-\mu} - 1] \sum_{\mathbf{q}_1, \mathbf{q}_2} f_{\mathbf{q}_1} (1 + f_{\mathbf{q}_1 + \mathbf{q}_2 - \mathbf{q}}) f_{\mathbf{q}_2} \delta(\omega + \varepsilon_{\mathbf{q}_1 + \mathbf{q}_2 - \mathbf{q}} - \varepsilon_{\mathbf{q}_1} - \varepsilon_{\mathbf{q}_2}). \quad (49)$$

Considering quadratic spectrum $\varepsilon_{\mathbf{q}} = \frac{q^2}{2m}$ for reservoir particles and passing to continuum limit with dimensionless momentum $q \rightarrow q\lambda_{dB}$, we obtain:

$$\Im[\Sigma_{\mathbf{q}}^+(\omega)] = -2 \frac{\pi V_0^2}{(2\pi)^4 \lambda_{dB}^4} [e^{\omega-\mu} - 1] \int d^2 \mathbf{q}_1 \int d^2 \mathbf{q}_2 \delta(\omega + (\mathbf{q}_1 + \mathbf{q}_2 - \mathbf{q})^2 - \mathbf{q}_1^2 - \mathbf{q}_2^2) f(q_1^2) [1 + f((\mathbf{q}_1 + \mathbf{q}_2 - \mathbf{q})^2)] f(q_2^2) \quad (50)$$

It's now helpful to use $q_+ = \frac{\mathbf{q}_1 + \mathbf{q}_2}{2}$ and $q_- = \mathbf{q}_1 - \mathbf{q}_2$ as integration variables:

$$\begin{aligned} \Im[\Sigma_{\mathbf{q}}^+(\omega)] = & -2 \frac{\pi V_0^2}{(2\pi)^4 \lambda_{dB}^4} [e^{\omega-\mu} - 1] \int d^2 \mathbf{q}_+ \int d^2 \mathbf{q}_- \delta\left(2q_+^2 - \frac{q_-^2}{2} - 4\mathbf{q}\mathbf{q}_+ + \omega + q^2\right) f_B\left[\left(\mathbf{q}_+ - \frac{\mathbf{q}_-}{2}\right)^2\right] \\ & \times \left(1 + f_B\left[(2\mathbf{q}_+ - \mathbf{q})^2\right]\right) f_B\left[\left(\mathbf{q}_+ + \frac{\mathbf{q}_-}{2}\right)^2\right] \end{aligned} \quad (51)$$

After integrating out the delta-function:

$$\begin{aligned} \Im[\Sigma_{\mathbf{q}}^+(\omega)] = & -\frac{V_0^2}{(2\pi)^3 \lambda_{dB}^4} [e^{\omega-\mu} - 1] \int_0^\infty d^2 \mathbf{q}_+ \int_0^\infty d^2 \mathbf{n}_- \Theta(2q_+^2 - 4\mathbf{q}\mathbf{q}_+ + \omega + q^2) \left(1 + f_B\left[(2\mathbf{q}_+ - \mathbf{q})^2\right]\right) \times \\ & f_B\left[2q_+^2 - 2\mathbf{q}\mathbf{q}_+ + \frac{\omega}{2} + \frac{q^2}{2} - \mathbf{n}_- \mathbf{q}_+ \sqrt{4q_+^2 - 8\mathbf{q}\mathbf{q}_+ + 2\omega + 2q^2}\right] f_B\left[2q_+^2 - 2\mathbf{q}\mathbf{q}_+ + \frac{\omega}{2} + \frac{q^2}{2} + \mathbf{n}_- \mathbf{q}_+ \sqrt{4q_+^2 - 8\mathbf{q}\mathbf{q}_+ + 2\omega + 2q^2}\right] \end{aligned} \quad (52)$$

Here $\mathbf{n}_- = \frac{\mathbf{q}_-}{q_-}$ is a unitary 2D vector. We now use $\mathbf{q}_\delta = \mathbf{q}_+ - \mathbf{q}$ and the corresponding unitary vector \mathbf{n}_δ to obtain:

$$\begin{aligned} \Im[\Sigma_{\mathbf{q}}^+(\omega)] = & -\frac{V_0^2}{(2\pi)^3 \lambda_{dB}^4} [e^{\omega-\mu} - 1] \int_0^\infty d^2 \mathbf{q}_\delta \int_0^\infty d^2 \mathbf{n}_- \Theta(2q_\delta^2 - q^2 + \omega) \left(1 + f_B\left[(2\mathbf{q}_\delta + \mathbf{q})^2\right]\right) \times \\ & f_B\left[2q_\delta^2(\mathbf{q} + \mathbf{q}_\delta) + \frac{\omega}{2} + \frac{q^2}{2} - \mathbf{n}_-(\mathbf{q} + \mathbf{q}_\delta) \sqrt{4q_\delta^2 - 2q^2 + 2\omega}\right] f_B\left[2q_\delta^2(\mathbf{q} + \mathbf{q}_\delta) + \frac{\omega}{2} + \frac{q^2}{2} + \mathbf{n}_-(\mathbf{q} + \mathbf{q}_\delta) \sqrt{4q_\delta^2 - 2q^2 + 2\omega}\right] \end{aligned} \quad (53)$$

The theta-function specifies lower integration limit as follows:

$$\begin{aligned} \Im[\Sigma_{\mathbf{q}}^+(\omega)] = & -\frac{V_0^2}{(2\pi)^3 \lambda_{dB}^4} [e^{\omega-\mu} - 1] \int d^2 \mathbf{n}_\delta \int d^2 \mathbf{n}_- \int_{\sqrt{\frac{q^2 - \omega}{2}}}^\infty q_\delta dq_\delta \left(1 + f_B\left[4q_\delta^2 + q^2 + 4z\mathbf{q}\mathbf{n}_\delta\right]\right) \times \\ & f_B\left[2q_\delta^2 + 2z\mathbf{n}_\delta \mathbf{q} + \frac{\omega + q^2}{2} - \mathbf{n}_-(\mathbf{q} + q_\delta \mathbf{n}_\delta) \sqrt{4q_\delta^2 - 2q^2 + 2\omega}\right] f_B\left[2z^2 + 2q_\delta \mathbf{n}_\delta \mathbf{q} + \frac{\omega + q^2}{2} + \mathbf{n}_-(\mathbf{q} + q_\delta \mathbf{n}_\delta) \sqrt{4q_\delta^2 - 2q^2 + 2\omega}\right] \end{aligned} \quad (54)$$

Now introduce angles $\mathbf{n}_- \mathbf{n}_q = \cos(\alpha_-)$, $\mathbf{n}_\delta \mathbf{n}_q = \cos(\alpha_\delta)$, $\mathbf{n}_- \mathbf{n}_\delta = \cos(\alpha_\delta - \alpha_-)$:

$$\begin{aligned} \Im[\Sigma_{\mathbf{q}}^+(\omega)] = & -\frac{V_0^2}{(2\pi)^3 \lambda_{dB}^4} [e^{\omega-\mu} - 1] \frac{1}{2} \int_0^{2\pi} d\alpha_- \int_0^{2\pi} d\alpha_\delta \int_{\sqrt{\frac{q^2 - \omega}{2}}}^\infty dq_\delta q_\delta \left(1 + f_B\left[4z^2 + q^2 + 4zq \cos(\alpha_\delta)\right]\right) \times \\ & f_B\left[2z^2 + 2zq \cos(\alpha_\delta) + \frac{\omega + q^2}{2} - [q \cos(\alpha_-) + q_\delta \cos(\alpha_\delta - \alpha_-)] \sqrt{4q_\delta^2 - 2q^2 + 2\omega}\right] \times \\ & f_B\left[2z^2 + 2zq \cos(\alpha_\delta) + \frac{\omega + q^2}{2} + [q \cos(\alpha_-) + q_\delta \cos(\alpha_\delta - \alpha_-)] \sqrt{4q_\delta^2 - 2q^2 + 2\omega}\right] = \frac{V_0^2}{(2\pi)^3 \lambda_{dB}^4} I_q(\omega) \end{aligned} \quad (55)$$

These expression may be used for evaluating $I_q(\omega)$. However, asymptotic behaviour may be studied analytically. Considering $\omega \rightarrow \infty$:

$$I_q(\omega \rightarrow \infty) = - [e^{\omega-\mu}] \int_0^{2\pi} d\alpha_- \int_0^{2\pi} d\alpha_+ \int_0^\infty dq_+ q_+ \frac{e^{\mu-\omega}}{e^{-\mu+4q_+^2} - 1} = -\frac{\pi^2}{2} \int_0^\infty dz \frac{1}{e^{-\mu+z} - 1} = -\frac{\pi^2}{2} \ln(1 - e^\mu) \quad (56)$$

The opposite limit $\omega \rightarrow \infty$ (note that $q \sim 1$ is a thermal momentum):

$$I(\omega \rightarrow \infty) = -[-1] \int_0^{2\pi} d\alpha_- \int_0^{2\pi} d\alpha_\delta \int_{\sqrt{-\frac{\omega}{2}}}^{\infty} dq_\delta q_\delta e^{2\mu - \omega - 4q_\delta^2} = 4\pi^2 \frac{e^{2\mu + \omega}}{8} = \frac{\pi^2}{2} e^{2\mu + \omega}. \quad (57)$$

Note that these asymptotic expressions are independent of q .

B Stability analysis

B.1 Stationary points. Stability

For stability analysis, we need to express equations in a form of an ODE system:

$$\dot{V} = -\frac{V^2}{2} - \left(\frac{\Gamma}{2} + \gamma\right) V + 2\nu(\nu - \varepsilon - ge^r) + \left(2\Lambda^+ \frac{\mu}{\gamma} - \gamma\Gamma\right) \quad (58)$$

$$\dot{r} = V \quad (59)$$

$$\dot{\nu} = -\frac{3}{2}V\nu + (\varepsilon + 2ge^r)V + \left(\frac{V}{2} - \gamma\right)(\nu - \varepsilon - ge^r) - \frac{1}{2}\Gamma\nu - \Lambda^+. \quad (60)$$

We may linearise it by substitution $\nu = \nu_{\text{eq}} + \delta\nu$, $V = \delta V$, $r = r_{\text{eq}} + \delta r$. Leaving first order terms only:

$$\dot{V} = -\left(\frac{\Gamma}{2} + \gamma\right)V + 2\delta\nu(\nu - \varepsilon - g\rho) + 2\nu(\delta\nu - g\rho\delta r), \quad (61)$$

$$\delta\dot{r} = V, \quad (62)$$

$$\delta\dot{\nu} = -\frac{3}{2}V\nu + (\varepsilon + 2g\rho)V - \gamma(\delta\nu - g\rho\delta r) + \left(\frac{V}{2}\right)(\nu - \varepsilon - g\rho) - \frac{1}{2}\Gamma\delta\nu. \quad (63)$$

Seeking the eigenmodes of this system in a form

$$\begin{pmatrix} V \\ \delta r \\ \delta\nu \end{pmatrix} = \begin{pmatrix} \delta V_0 \\ \delta r_0 \\ \delta\nu_0 \end{pmatrix} e^{\chi t},$$

leads to the following characteristic equation:

$$\begin{vmatrix} -\left(\frac{\Gamma}{2} + \gamma\right) - \chi & -2g\rho\nu & 2(2\nu - \varepsilon - g\rho) \\ 1 & -\chi & 0 \\ \left(\frac{\varepsilon}{2} + \frac{3}{2}g\rho - \nu\right) & \gamma g\rho & -\left(\frac{\Gamma}{2} + \gamma\right) - \chi \end{vmatrix} = 0. \quad (64)$$

Denoting $f^2 = \left(\gamma + \frac{\Gamma}{2}\right)^2 + (\varepsilon - 2\nu + g\rho)^2 + 2g\rho(\varepsilon - \nu + g\rho)$, we may rewrite it as a cubic equation with respect to the eigenvalue χ :

$$\chi^3 + (2\gamma + \Gamma)\chi^2 + f^2\chi + 2g\rho[\Gamma\nu + \Lambda^+] = 0 \quad (65)$$

Using expressions () for the stationary points, one may simplify (+ sign in the last term corresponds to the upper stationary point):

$$\chi^3 + (2\gamma + \Gamma)\chi^2 + f_\pm^2\chi \pm 2g\rho_\pm\sqrt{D} = 0 \quad (66)$$

with f_\pm^2 being expressed as:

$$f_\pm^2 = \left(\gamma + \frac{\Gamma}{2}\right)^2 + \frac{\left[(2\gamma + \Gamma)\Lambda^+ \mp (2\gamma - \Gamma)\sqrt{D}\right]^2}{4\gamma^2\Gamma^2} + \frac{g\rho_\pm}{\gamma}(\Lambda^+ \pm \sqrt{D}). \quad (67)$$

First note that whenever the lower stationary point exists ($D > 0$ and $\rho_- \geq 0$) the free term on the left-hand side of (66) is negative. It is enough to conclude that the lower solution has at least one positive real eigenvalue $\chi > 0$ leading to instability.

For the upper stationary point, all the terms are positive whenever it exists. Therefore, the cubic equation (66) has one real negative eigenvalue and two complex-conjugate eigenvalues. We may explicitly consider the real and imaginary components of $\chi = \kappa + i\Omega$, which leads to the following equation system:

$$\begin{cases} \kappa^3 + (\kappa^2 - \Omega^2)(2\gamma + \Gamma) + \kappa(f_{\pm}^2 - 3\Omega^2) \pm 2g\rho_{\pm}\sqrt{D} = 0 \\ \Omega[3\kappa^2 - \Omega^2 + 2\kappa(2\gamma + \Gamma) + f_{\pm}^2] = 0 \end{cases} \quad (68)$$

The non-zero frequency satisfying the second equation is $\Omega^2 = 3\kappa^2 + 2\kappa(2\gamma + \Gamma) + f_{\pm}^2$. By substitution, we get:

$$\kappa^3 + (2\gamma + \Gamma)\kappa^2 + \left(\left(\gamma + \frac{\Gamma}{2} \right)^2 + \frac{f_{\pm}^2}{4} \right) \kappa + \frac{1}{4} \left(\gamma + \frac{\Gamma}{2} \right) f_{\pm}^2 \mp \frac{g\rho_{\pm}}{4} \sqrt{D} = 0 \quad (69)$$

The free term here may be expressed as follows:

$$\begin{aligned} \frac{1}{4} \left(\gamma + \frac{\Gamma}{2} \right) f_{\pm}^2 \mp \frac{g\rho_{\pm}}{4} \sqrt{D} &= \frac{1}{4} \left(\gamma + \frac{\Gamma}{2} \right) \left[\left(\gamma + \frac{\Gamma}{2} \right)^2 + \frac{[(2\gamma + \Gamma)\Lambda^+ \mp (2\gamma - \Gamma)\sqrt{D}]^2}{4\gamma^2\Gamma^2} + \frac{g\rho_{\pm}}{\gamma} (\Lambda^+ \pm \sqrt{D}) \right] \mp \frac{g\rho_{\pm}}{4} \sqrt{D} = \\ &= \frac{1}{4} \left(\gamma + \frac{\Gamma}{2} \right)^3 + \frac{1}{4} \left(\gamma + \frac{\Gamma}{2} \right) \frac{[(2\gamma + \Gamma)\Lambda^+ \mp (2\gamma - \Gamma)\sqrt{D}]^2}{4\gamma^2\Gamma^2} + \frac{g\rho_{\pm}}{8\gamma} [(2\gamma + \Gamma)\Lambda^+ \pm \Gamma\sqrt{D}]. \end{aligned}$$

We may now note that all the coefficients of the cubic equation (69) are positive for + sign chosen, which leads to $\kappa < 0$ and allows to finally conclude that the upper stationary point is stable.

B.2 Decaying solutions

We start from the characteristic equations for the decaying solution, presented in the main text:

$$\begin{cases} \frac{\kappa^2}{2} = - \left(\frac{\Gamma}{2} + \gamma \right) \kappa + \left(2\frac{\mu}{\gamma}\Lambda^+ - \gamma\Gamma \right) + 2\Omega(\Omega - \varepsilon), \\ 0 = -\frac{3}{2}\kappa\Omega + \varepsilon\kappa + \left(\frac{\kappa}{2} - \gamma \right) (\Omega - \varepsilon) - \frac{1}{2}\Gamma\Omega - \Lambda^+. \end{cases} \quad (70)$$

After excluding ν from these equations and using a substitution $\kappa \rightarrow -\gamma - \frac{\Gamma}{2} + y$:

$$\Omega = \frac{\varepsilon \left(\gamma + \frac{\kappa}{2} \right) - \Lambda^+}{\kappa + \gamma + \frac{\Gamma}{2}}, \quad (71)$$

$$f(y) = y^4 + \left(\varepsilon^2 - \left(\gamma - \frac{\Gamma}{2} \right)^2 - 4\Lambda^+ \frac{\mu}{\gamma} \right) y^2 - \left(\left(\gamma - \frac{\Gamma}{2} \right) \varepsilon - 2\Lambda^+ \right)^2 = 0. \quad (72)$$

Since the last term is given by subtraction of a non-negative perfect square, in order for all the roots to be less than $\gamma + \frac{\Gamma}{2}$ (which is the same as requesting all the κ s to be negative), we need to impose a condition $f\left(\frac{\Gamma}{2} + \gamma\right) \geq 0$. By direct substitution, one may verify that this stability condition is equivalent to the inequality

$$\left(\frac{\rho_+ + \rho_-}{2} \right)^2 \geq \left(\frac{\rho_+ - \rho_-}{2} \right)^2 = \left(\frac{1}{\Gamma} + \frac{1}{2\gamma} \right)^2 \frac{D}{g^2} \quad (73)$$

or $\rho_+\rho_- \geq 0$. From the expression above, we see that $D < 0$ (when there are no stationary points at all) also satisfies the stability condition. The eigenvalues themselves are of the following form:

$$\kappa_{\pm} = -\gamma - \frac{\Gamma}{2} \pm \frac{\sqrt{2} \sqrt{\sqrt{\left(\varepsilon^2 - \left(\gamma - \frac{\Gamma}{2} \right)^2 - 4\Lambda^+ \frac{\mu}{\gamma} \right)^2 + 4 \left(\left(\gamma - \frac{\Gamma}{2} \right) \varepsilon - 2\Lambda^+ \right)^2} - \left(\varepsilon^2 - \left(\gamma - \frac{\Gamma}{2} \right)^2 - 4\Lambda^+ \frac{\mu}{\gamma} \right)}}{2} = -\gamma - \frac{\Gamma}{2} \pm \frac{\Delta\kappa}{2}. \quad (74)$$

The corresponding frequencies are:

$$\Omega_{\pm} = \frac{\varepsilon \left(\gamma + \frac{\kappa}{2} \right) - \Lambda^+}{\kappa + \gamma + \frac{\Gamma}{2}} = \frac{\varepsilon}{2} \mp \frac{\varepsilon(\gamma - \Gamma) - 2\Lambda^+}{\Delta\kappa}. \quad (75)$$

References

- [1] S. Bose, Z. Phys. **26**, 178 (1924).
- [2] A. Einstein, Sitz. ber. Preuss. Akad. Wiss. **1**, 3-14 (1925).
- [3] M.H. Anderson, J.R. Ensher, M.R. Matthews, C.E. Wieman, and E.A. Cornell, Science **269**, 198201 (1995).
- [4] C.C. Bradley, C.A. Sackett, J.J. Tollett, and R.G. Hulet, Phys. Rev. Lett. **75**, 1687 (1995).;
- [5] K.B. Davis et al., Phys. Rev. Lett. **75**, 39693973 (1995).
- [6] A. A. High, J. R. Leonard, A. T. Hammack, M. M. Fogler, L. V. Butov, A. V. Kavokin, K. L. Campman et A. C. Gossard Nature **483**, 584–588 (2012).
- [7] A. A. High, J. R. Leonard, A. T. Hammack, M. M. Fogler, L. V. Butov, A. V. Kavokin, K. L. Campman et A. C. Gossard Nano Lett., **12**, 5 (2012).
- [8] J.Kasprzak et al., Nature **443**, 409 (2006).
- [9] R.Balili et al., Science **316**, 1007 (2007).
- [10] S.O. Demokritov et al., Nature **443**, 430 (2006).
- [11] J.Klaers, J.Schmitt, F.Verwinger, and M.Weitz, Nature **468**, 545 (2010).
- [12] A. Imamoglu, R.J. Ram, Physics Letters A **214**, Volume 214, Issues 3–4, Pages 193-198 (1996).
- [13] C. Piermarocchi, F. Tassone, V. Savona, A. Quattropani, and P. Schwendimann Phys. Rev. B **53**, 15834 (1996).
- [14] P. Stenius Physics Letters B **60**, 14072 (1999)
- [15] M. Wouters and I. Carusotto, Phys. Rev. Lett. **99**, 140402 (2007) PPhys. Rev. Lett. **99**, 140402 (2007)
- [16] J. Keeling, N. G. Berloff, Phys. Rev. Lett. **100**, 250401(2008)
- [17] F. Manni, K. G. Lagoudakis *et al*, Phys. Rev. Lett. **107**, 106401 (2011).
- [18] A. Opala, M. Pieczarka, and M. Matuszewski, Phys. Rev. B **98**, 195312 (2018).
- [19] L. P. Pitaevskii, Sov. Phys. JETP **35**, 282 (1959).
- [20] M. Wouters and I. Carusotto, Phys. Rev. Lett. **105**, 020602 (2010).
- [21] H. Haug, T. D. Doan, and D. B. Tran Thoai Phys. Rev. B **89**, 155302 (2014).
- [22] A. A. Elistratov and Yu. E. Lozovik Phys. Rev. B **97**, 014525 (2018).
- [23] H. T. C. Stoof, arxiv.org/cond-mat/9805393
- [24] H. T. C. Stoof, [arXiv:cond-mat/9910441](https://arxiv.org/cond-mat/9910441).
- [25] A.-W. de Leeuw, H. T. C. Stoof, and R. A. Duine Phys. Rev. B **88**, 033829 (2013).
- [26] Phys. Rev. B **93**, 195306 (2016)
- [27] A. O. Slobodeniuk and D. M. Basko Phys. Rev. B **94**, 205423 (2016).
- [28] H.T.C. Stoof, Phys. Rev. Lett. **66**, 3148 (1991);Phys. Rev. A **45**, 8398 (1992).